Characterization of a Bioprosthetic Bicuspid Venous Valve Hemodynamics: Implications for Mechanism of Valve Dynamics

W.-H. Tien [b], H.Y. Chen [a,d,e], Z.C. Berwick [a,d], J. Krieger [f], S. Chambers [f], D. Dabiri [b], G.S. Kassab [c,d,e,*]

[a] Research and Development, 3DT Holdings, LLC, Indianapolis, IN, USA
[b] Department of Aeronautics and Astronautics, University of Washington, Seattle, WA, USA
[c] Department of Surgery, Indiana University School of Medicine, Indianapolis, IN, USA
[d] Department of Cellular and Integrative Physiology, Indiana University School of Medicine, Indianapolis, IN, USA
[e] Department of Biomedical Engineering, IUPUI, Indianapolis, IN, USA
[f] Research Engineering, COOK® Medical, Bloomington, IN, USA

WHAT THIS PAPER ADDS

We present both experimental and simulation results to highlight the performance of a prosthetic venous valve. The findings enhance our understanding of the function of native venous valve and the design of a prosthetic venous valve for potential treatment of chronic venous inefficiency.

Background: Chronic venous insufficiency (CVI) of the lower extremities is a common clinical problem. Although bioprosthetic valves have been proposed to treat severe reflux, clinical success has been limited due to thrombosis and neointima overgrowth of the leaflets that is, in part, related to the hemodynamics of the valve. A bioprosthetic valve that mimics native valve hemodynamics is essential.

Methods: A computational model of the prosthetic valve based on realistic geometry and mechanical properties was developed to simulate the interaction of valve structure (fluid—structure interaction, FSI) with the surrounding flow. The simulation results were validated by experiments of a bioprosthetic bicuspid venous valve using particle image velocimetry (PIV) with high spatial and temporal resolution in a pulse duplicator (PD).

Results: Flow velocity fields surrounding the valve leaflets were calculated from PIV measurements and comparisons to the FSI simulation results were made. Both the spatial and temporal results of the simulations and experiments were in agreement. The FSI prediction of the transition point from equilibrium phase to valve-closing phase had a 7% delay compared to the PD measurements, while the PIV measurements matched the PD exactly. FSI predictions of reversed flow were within 10% compared to PD measurements. Stagnation or stasis regions were observed in both simulations and experiments. The pressure differential across the valve and associated forces on the leaflets from simulations showed the valve mechanism to be pressure driven.

Conclusions: The flow velocity simulations were highly consistent with the experimental results. The FSI simulation and force analysis showed that the valve closure mechanism is pressure driven under the test conditions. FSI simulation and PIV measurements demonstrated that the flow behind the leaflet was mostly stagnant and a potential source for thrombosis. The validated FSI simulations should enable future valve design optimizations that are needed for improved clinical outcome.

Article history: Received 18 March 2014, Accepted 7 June 2014, Available online 21 August 2014

Keywords: Bioprosthetic valve, Venous flow, Chronic venous inefficiency, Fluid-structure interaction, Particle image velocimetry

INTRODUCTION

Chronic venous insufficiency (CVI) of lower extremities is a common clinical problem, which constitutes 2% of the total Western society health-care budget. The main cause is that the venous valves of the patients become incompetent resulting in venous reflux and distal venous hypertension. The venous insufficiency can be primary (idiopathic) or secondary (post-thrombotic). Secondary venous insufficiency is primarily caused by deep vein thrombosis (DVT) or trauma.[1]

Current management of patients with chronic deep venous incompetence (CDVI) is limited to strategies that manage symptoms. Prosthetic valve implantation is one proposed alternative for treating CDVI, which may restore all or part of the function of the native venous valve. Although several valve designs had been proposed in the last decade,[2–4] long-term durability and thrombosis remain as major hurdles. The validation of computational simulations that enable future

* Corresponding author. Ghassan S. Kassab, Ph.D., California Medical Innovations Institute, 11107 Roselle St., San Diego, CA 92121, USA. Tel.: +1 858 249 7418 (Office), +1 858 999 5235 (Cell).
E-mail address: gkassab@iupui.edu (G.S. Kassab).

1078-5884/$ — see front matter
http://dx.doi.org/10.1016/j.ejvs.2014.06.034

valve design optimization is needed to avoid empirical design iterations that are costly in time and resources.

The phasic nature of venous flow makes the flow dynamics highly interactive with the leaflets. Owing to the large deformation of leaflets and the strong interaction between leaflets and blood, fluid—structure interaction (FSI) simulations are necessary to understand the full dynamics of such complex interactions.[5,6] Recently, the FSI simulation has been successfully applied to compare valve architectures (mono-, bi-, and tricuspid) and the implications of these designs on the fluid and solid mechanics of the valve leaflets.[7]

Particle image velocimetry (PIV) is a powerful *in vitro* technique to resolve flow fields with high spatial resolution for cardiovascular studies. Several groups have applied this technique to measure flow fields around mechanical, prosthetic, or native aortic valves,[8—10] but results in these studies are not applicable to venous flow. Using echo speckles of red blood cells (RBCs) as flow tracers, Nam et al.[11] applied the velocimetry technique with a high-frequency ultrasound system (HFUS) to image the motions of valve cusps and vortices behind the sinus pocket at the perivalvular area in a human superficial vein. The resolvable flow velocity of HFUS was limited to 4.2 mm/s due to the 30-Hz frame rate, which is much lower than the peak velocity (18.2 cm/s) reported by Lurie et al.[12] in patients. For studying the fluid dynamics around the prosthetic venous valves, the PIV technique has recently been applied to study the effect of the sinus and the coupling dynamics between a pair of valves.[13,14] The major drawback of this technique is the lack of fluid or solid stresses data.

The main objective of the current study was to validate a FSI simulation method that can fully simulate the coupling dynamics to characterize the fluid dynamics of a bioprosthetic bicuspid venous valve. An *in vitro* PIV system was used to validate the FSI model, which was then used to determine the pressure and forces acting on the valve to reveal the mechanism of valve dynamics as likely pressure driven rather than flow driven under the test conditions.[12] The combination of experiments and simulations also serve as virtual testing tools to optimize the design of a bioprosthetic venous valve.

MATERIALS AND METHODS

Computational methods of FSI simulation model

The FSI methods were detailed in a previous publication.[7] The fluid domain is governed by the Navier—Stokes and continuity equations as expressions of laws of physics. The solid domain is governed by the momentum and equilibrium equations. Further details of the numerical methods have been described in previous publications.[5,7]

In vitro *experimental set-up of PIV*

The *in vitro* experimental set-up using the PIV technique is described in detail in our previous publications.[13,14] Fluorescent tracer particles seeded to the test section emit lights from the pulsed laser light source and was recorded by a charge-coupled device (CCD) camera for calculating the local flow velocities. Image pairs were first pre-processed to remove the valve area and the unwanted reflections. Each pre-processed image pair was then divided into interrogation sub-windows to be processed by cross-correlation PIV algorithms to find the mean particle velocity inside each interrogation window.[15] The outlier filter[16] was a median filter normalized by the median of the neighboring velocity residuals, and the outliers were then replaced by interpolating the neighboring vectors.

Experimental conditions

The mean flow rate was set at 0.35 L/min at 15 beats per minute, with the peak flow rate at 1.1 L/min and the peak inflow pressure at 40 mmHg. This is in agreement with the flow range in a normal human based on previous studies.[17—19]

Working fluid

In the flow scale in this study, the particulate behavior of individual cells is insignificant because the vessel is much larger than individual blood cells. The fluid mechanical behavior of blood can therefore be approximated by a viscous fluid. The working fluid was a solution of glycerol and water at a volume ratio of 2:3. The resultant viscosity at 25 °C was 3.66 CSt, and the Reynolds and Womersley numbers were 358.5 and 4.47, respectively.

Prosthetic valve

The bioprosthetic valve used for the *in vitro* PIV experiments in this study was provided by Cook Biotech Inc. (West Lafayette, IN, USA; Fig. 1). The valve was a third-generation bioprosthetic venous valve (BVV3) frame with a 12 mm nominal diameter. The valve is a bicuspid design to mimic a native venous valve. Fixed tissues cut into leaflet shape were sutured onto a shape memory nitinol frame that can be deployed with a catheter system. More detail can be found in Pavcnik et al.[4]

RESULTS

Hemodynamic results

The flow and pressure data of the valve are shown in Fig. 2, where the four phases of the valve cycle[12] can be identified

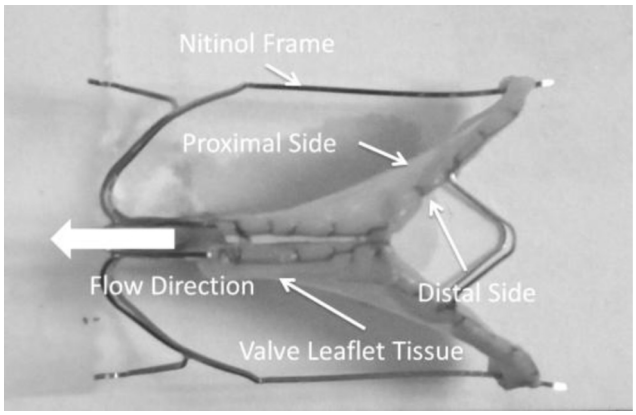

Figure 1. The bioprosthetic valve used in the studies.

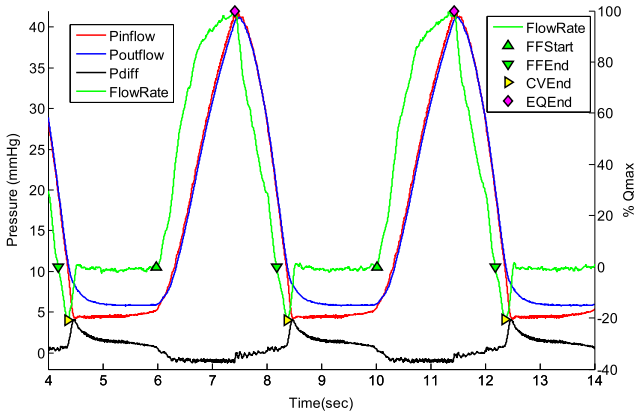

Figure 2. Valve log of the PIV experiment processed using MATLAB. Red line: valve inflow pressure. Blue line: outflow pressure. Green line: flow rate. Black line: pressure difference between inflow and outflow pressure. FFStart (upward-pointing green triangles): start of forward flow. FFEnd (downward-pointing green triangles): end of forward flow. EQEnd (magenta diamond): End of equilibrium. CVEnd (yellow triangle): end of closing volume.

and described as follows. The bulk flow rate increases until it reaches a peak value (from FFStart to EQEnd), and the rate of increase can be identified with two different slopes. This period is the opening phase and the equilibrium phase, separated by the change of the slope of the flow rate. The flow rate then decreases to a negative peak value and the pressure difference increases (from EQEnd to CVEnd). This period is the valve-closing phase, since the flow rate is reducing. The flow rate then stabilizes around zero until the end of the cycle, and the pressure difference starts to build up after the flow rate reaches the minimum magnitude (from CVEnd to FFStart). This period is the valve-closed phase, since the valve is closed and flow is stopped by the valve which increases the pressure difference.

PIV–FSI comparison

Representative figures of the resolved velocity field are overlaid with vorticity field from the PIV experiments and the FSI simulation in Fig. 3A and B, respectively. The PIV results showed that the flow is stagnant at the proximal side of the leaflets. The lack of valve sinus likely prevented vortices formation. As the valve closes, the leaflets collapse in response to the adverse (negative) pressure gradient and form coaptation to stop the flow. Both the PIV and the FSI show that a jet forms at the exit of the valve, while the pocket regions had extensive stagnation regions.

The comparison of the temporal flow rate waveform from the pulse duplicator, PIV, and FSI simulation is shown in Fig. 4A. PD and PIV traces matched very closely with each other, as expected, since both are measuring the same apparatus and flow. A good agreement between the FSI

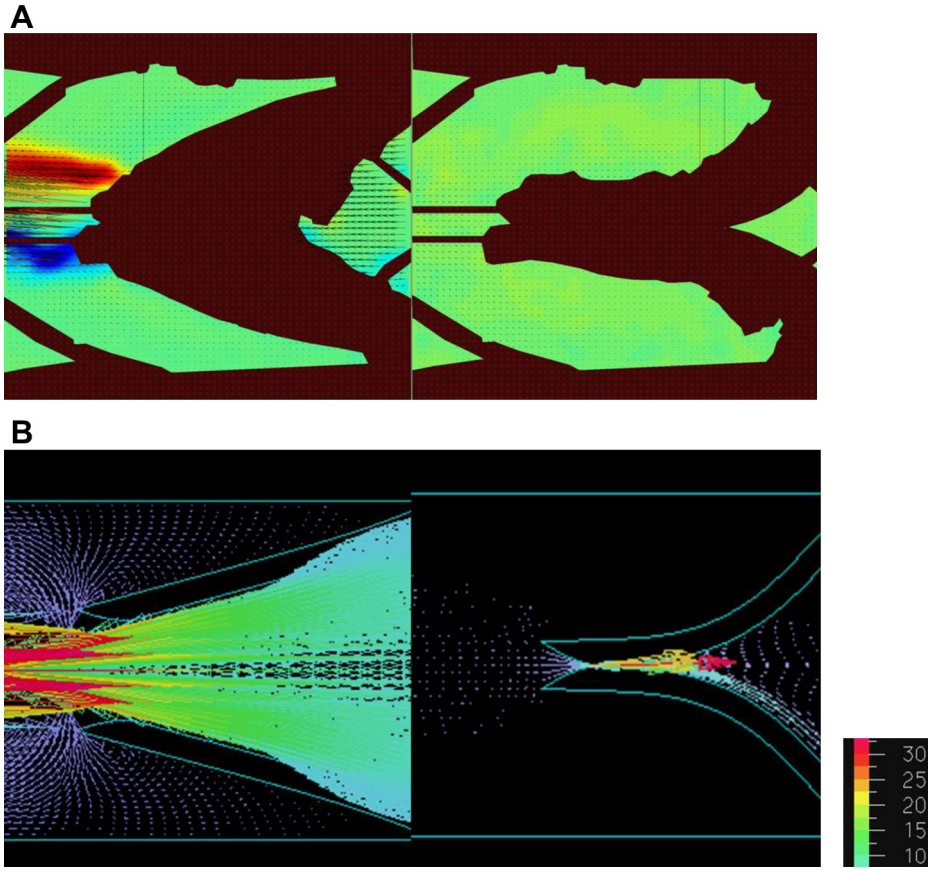

Figure 3. (A) The PIV velocity field and vorticity. (B) The FSI flow field during opening and closed stages. Both the PIV and FSI showed that a jet formed at the exit of valve, while the sinus regions had extensive stagnation. The test valve had a degree of asymmetry. The velocity color scale is in cm/s. The quantitative comparisons are in Fig. 4.

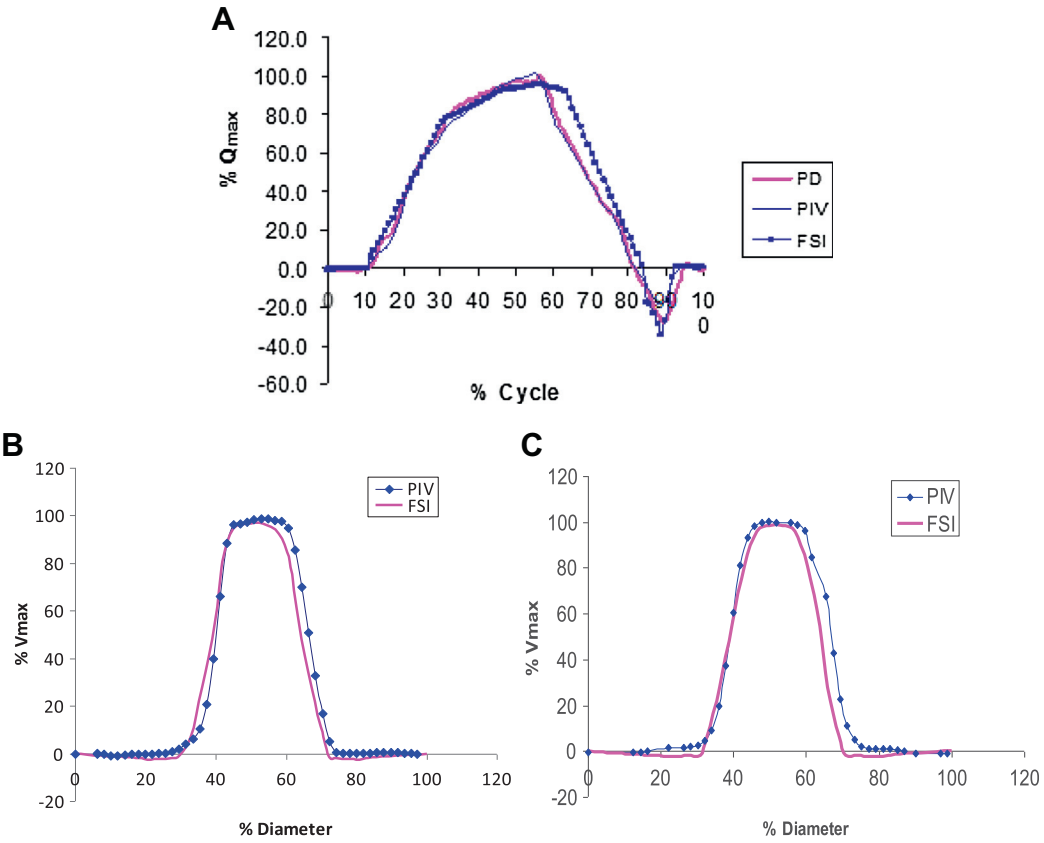

Figure 4. (A) The comparison of flow rate waveforms from pulse duplicator (measured by standard flow meter), PIV and FSI simulation. The transient dynamics of the output waveforms were similar. (B,C) Comparisons of flow velocity profiles measured by PIV and simulated from FSI. Detailed descriptions are in the associated text.

results and the PD and PIV measurements was also observed. The transient dynamics of the waveforms were similar. The reverse flow during the final stage of closure was also predicted by the FSI simulation. The FSI prediction of the transition point from equilibrium phase to valve-closing phase had a 7% delay compared to the PD log, while the PIV measurements matched the PD log exactly. Furthermore, the FSI prediction of reversed flow compared to PD measurements were within 10% agreement.

Comparisons of flow velocity profiles at cross-sections measured by PIV and simulated from FSI are shown in Fig. 4B,C. Fig. 4B and C are flow velocity profiles at cross-sections perpendicular to the flow at 1 and 2 mm downstream from the leaflet tips. The velocity profile was plotted as a function of % diameter. 0% diameter is at the vein wall, 50% is at the center of lumen, and 100% is at the opposite vein wall. The velocity profiles obtained from PIV and FSI results were very similar.

Force analysis of FSI model

Fig. 5 shows the force analysis results of the FSI simulations. Fig. 5A shows the pressure difference between the proximal and distal side of the valve leaflet at different leaflet locations. The pressure difference increases at the start of the cycle, reaches a peak value, and then decreases to become negative after valve closure. This result matches very well to the four valve phases: opening, equilibrium, closing, and full closing.[12] During opening, the pressure difference was the largest at the leaflet base (hinge) and smallest at the tip. After closing, the pressure difference became the same at the base, middle and tip. The force on the leaflet shows a similar trend as the pressure differential (Fig. 5B). The force increased during opening, decreased during closing and became negative after closing.

DISCUSSION

Validation of FSI simulation model

The comparisons in Fig. 4 show good agreements between the experimental PIV and PD methods and the computational FSI simulation model. High flow velocities were observed at the center of the lumen, while flow velocities decreased towards the wall, as expected. Owing to the asymmetry of the test valve, the velocity profile skewed off center and was not completely symmetric. In summary, the temporal and spatial comparisons between FSI and PIV were reasonable and the transient dynamics were highly consistent.

Similarities and differences to native valves

The flow characteristics are similar to the native valve case, with a noticeable difference. Lurie et al.[12,20] investigated the venous valve closure mechanism on healthy volunteers under normal physiological conditions using duplex ultrasound

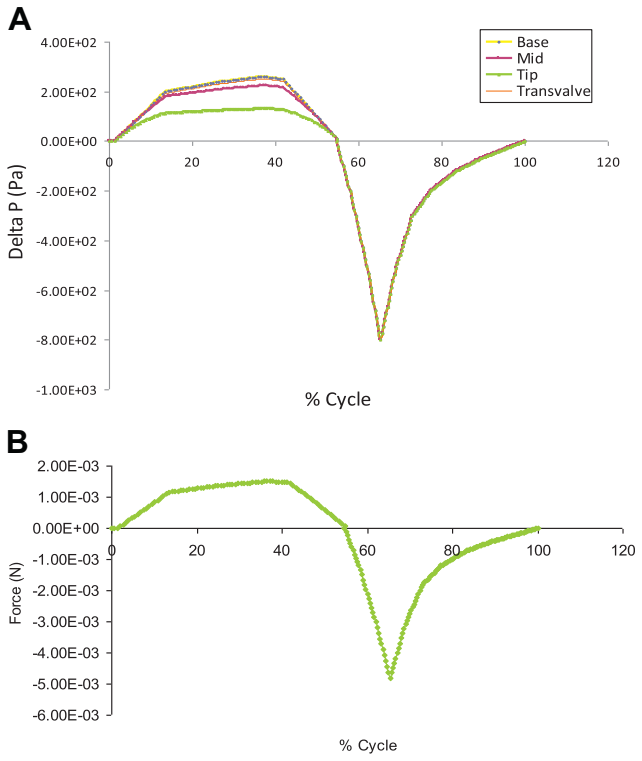

Figure 5. (A) The pressure differential across the valve increased during opening, decreased during closing and became negative after closure. The delta P at leaflet base (hinge) was largest while it is the least at the tip during opening and closing. After closure, the delta P became about the same at the base, middle and tip. The delta P pre- and post-valve was similar to delta P at leaflet base. (B) The overall force on the leaflet shows a similar trend as delta P.

imaging. Flow separation at the leading edge of the cusp and reattachment at the wall of the sinus were observed. They concluded that the vortical flow in the sinus region plays an important role in the valve operation and prevents stasis inside the valve pocket. Owing to the resolution limitation of the ultrasound imaging, there was no detailed flow field information to show the vortex behind the leaflet.

The present findings reflect similarities and differences between native and prosthetic valves. Since the bicuspid design of the prosthetic valve mimics the general structure of the native valve, the bulk flow around the prosthetic valve is similar to that of a native valve. There were three differences between the implant prosthetic valve and the native valve that, however, can alter the local flow patterns around the valve. First, the lack of sinus and hence the space behind the leaflet was small such that the valve reached its equilibrium stage without the vortex presented behind the leaflet. Second, the valve leaflets were different in material and geometry. Third, the attachment of the valve to the vessel wall was different. For the prosthetic valve, the attachment of the valve to the vessel was through the nitinol frame. Since the valve leaflets and vein vessel deform significantly during valve phases, the last two differences play significant roles in changing the valve opening geometry that affects the local flow characteristics.

Valve closure mechanism

In the early 1990s, van Bemmelen et al.[21] studied the venous dynamics based on *in vivo* measurements from healthy volunteers using B-mode echo imaging. The valve performance was investigated during the Valsalva maneuver, creating higher pressure proximal to the studied venous segment. Qui et al.[22] performed *in vitro* experimental studies on both stented and stentless bovine jugular valves. Velocity data were measured using laser Doppler velocimetry (LDV) on the valve inlet and 2 cm downstream of the valve to quantify flow reflux. The results did not confirm findings from van Bemmelen et al.[21] but suggested that the venous valve is a pressure differential-driven rather than a flow-driven device.

The results from both PIV experiments and FSI simulations suggest that the current prosthetic valve is driven by the pressure differential across the valve under the tested conditions. FSI simulations showed the pressure differential across the valve increased during opening, decreased during closing and became negative after closing (Fig. 5A). During opening, the P differential was largest at the leaflet base (hinge) and least at the tip. After closure, the P differential became the same at the base, middle, and tip, as the effects of flow at the various locations are minimized after closing. The force on the leaflet showed a very similar trend as the P differential (Fig. 5B). The force increased during opening, decreased during closing and became negative after closing. Additionally, the flow data showed that the flow rate started to decrease at about 55% of cycle, indicating the start of valve closing. This is significantly earlier than the negative flow which appeared later in the cycle (Fig. 4A). The negative flow is likely the result of final stage of valve closure, because the deformation of the closing valve created a volume change and the fluid behind the leaflet was squeezed backwards. The above findings are consistent with previous studies,[12,22] suggesting that the valve under the tested flow condition is pressure differential driven and venous reflux is not necessary for the valve to close. The flow reversal has been shown to lead to vascular dysfunction due to the reduction of nitric oxide concentration.[23,24] Clinical studies also show evidence of CVD progression due to abnormal venous reflux.[25]

Impacts on valve design

To prevent thrombosis, the leaflet geometry and motion must be optimized to minimize flow stagnation regions without leaflets contacting vessel wall. Since the leaflet is a fixed biologic graft material, the endothelialization of the valve is expected to initiate at leaflet base as the endothelial cells proliferate from the vein wall onto the valve. In order for the phenotype of the endothelial cells to be normal, the fluid shear stress and solid stress are key variables that must be within the physiological range. We have used the validated FSI simulations for evaluation of valve architectures based on endothelial shear stress and solid wall stress,[7] and proposed that valve design optimization can be achieved by minimizing the ratio of leaflet wall stress and fluid wall shear stress. A virtual design of valves is more efficient and less time-consuming than an empirical trial and error approach.

Limitations

The flow field in veins is complicated due to compliance of veins, variable arteriolar and venular resistance, influence of the surrounding muscular pump, and the phasic resistance imposed by respiration. External pressure from muscles may change vein geometry and the veins are highly compliant unlike the simplified glass tube models.

Under certain physiological conditions, the valve motion may be influenced by factors other than pressure difference. While the local muscle pump (calf muscle contraction) can generate pressure difference across the valve, there are other significant physiological and anatomical variables. For example, a change of position from supine to upright position can induce reflux because of the presence of gravity (hydrostatic column), and in turn induce the motion of the valve. The valve motion and flow structure under these circumstances are beyond the scope of this study.

CONCLUSIONS

The FSI spatial and temporal simulations of flow velocity were found to be in good agreement with the experimental results obtained from PIV. The FSI and PIV results were also compared and validated with the flow waveform from PD measurements. Both FSI and PIV results showed that the valve tested was a pressure-driven device and the presence of stagnation zones that may be a major source for thrombosis. The validated FSI simulations enable further design optimization for improved long-term outcome of the bioprosthetic valve, such as the profile of valve leaflets to avoid flow stagnation and reduce the risk factor of thrombosis and remodeling caused by endothelial shear and solid stress.

ACKNOWLEDGMENTS

This research was supported by 3DT Holdings, LLC and COOK® Medical. We wish to acknowledge the excellent technical expertise of Dr. Chad Johnson and Mrs. Martha Spicer.

REFERENCES

1 Bergan JJ, Schmid-Schonbein GW, Smith PD, Nicolaides AN, Boisseau MR, Eklof B. Chronic venous disease. *N Engl J Med* 2006;**355**(5):488—98.
2 de Borst GJ, Moll FL. Percutaneous venous valve designs for treatment of deep venous insufficiency. *J Endovasc Ther* 2012;**19**(2):291—302.
3 Zervides C, Giannoukas AD. Historical overview of venous valve prostheses for the treatment of deep venous valve insufficiency. *J Endovasc Ther* 2012;**19**(2):281—90.
4 Pavcnik D, Uchida B, Kaufman J, Hinds M, Keller FS, Rösch J. Percutaneous management of chronic deep venous reflux: review of experimental work and early clinical experience with bioprosthetic valve. *Vasc Med* 2008;**13**(1):75—84.
5 Chen HY, Navia JA, Kassab GS. Vessel-clamp interaction: transient closure dynamics. *Ann Biomed Eng* 2009;**37**(9):1772—80.
6 Anand M, Rajagopal K, Rajagopal KR. A model incorporating some of the mechanical and biochemical factors underlying clot formation and dissolution in flowing blood: review article. *J Theor Med* 2003;**5**(3—4):183—218.
7 Chen HY, Berwick Z, Krieger J, Chambers S, Lurie F, Kassab GS. Biomechanical comparison between mono-, bi-, and tricuspid valve architectures. *J Vasc Surg* **2**:188—93.e1.
8 Lim WL, Chew YT, Chew TC, Low HT. Pulsatile flow studies of a porcine bioprosthetic aortic valve in vitro: PIV measurements and shear-induced blood damage. *J Biomech* 2001;**34**(11):1417—27.
9 Li CP, Lo CW, Lu PC. Estimation of viscous dissipative stresses induced by a mechanical heart valve using PIV data. *Ann Biomed Eng* 2010;**38**(3):903—16.
10 Saikrishnan N, Yap CH, Milligan NC, Vasilyev NV, Yoganathan AP. In vitro characterization of bicuspid aortic valve hemodynamics using particle image velocimetry. *Ann Biomed Eng* 2012;**40**(8):1760—75.
11 Nam KH, Yeom E, Ha H, Lee SJ. Velocity field measurements of valvular blood flow in a human superficial vein using high-frequency ultrasound speckle image velocimetry. *Int J Cardiovasc Imaging* 2012;**28**(1):69—77.
12 Lurie F, Kistner RL, Eklof B, Kessler D. Mechanism of venous valve closure and role of the valve in circulation: a new concept. *J Vasc Surg* 2003;**38**(5):955—61.
13 Tien WH, Chen HY, Berwick Z, Krieger J, Chambers S, Dabiri D, et al. Role of sinus in prosthetic venous valve. *Eur J Vasc Endovasc Surg* 2014;**48**(1):98—104.
14 Tien WH, Chen HY, Berwick Z, Krieger J, Chambers S, Dabiri D, et al. Hemodynamic coupling of a pair of venous valves. *J Vasc Surg* **2**:303—14.
15 Raffel M, Kompenhans J, Wereley ST, Willert CE. *Particle image velocimetry: a practical guide*. 2nd ed. (Springer e-books.). Berlin: Springer-Verlag; 2007.
16 Westerweel J, Scarano F. Universal outlier detection for PIV data. *Exp Fluids* 2005;**39**(6):1096.
17 Meissner MH, Moneta G, Burnand K, Gloviczki P, Lohr JM, Lurie F, et al. The hemodynamics and diagnosis of venous disease. *J Vasc Surg* 2007;**46**(6):S4—24.
18 Fronek A, Criqui MH, Denenberg J, Langer RD. Common femoral vein dimensions and hemodynamics including Valsalva response as a function of sex, age, and ethnicity in a population study. *J Vasc Surg* 2001;**33**(5):1050—6.
19 Rittgers SE, Oberdier MT, Pottala S. Physiologically-based testing system for the mechanical characterization of prosthetic vein valves. *Biomed Eng Online* 2007;**6**(1):29.
20 Lurie F, Kistner RL, Eklof B. The mechanism of venous valve closure in normal physiologic conditions. *J Vasc Surg* 2002;**35**(4):713—7.
21 van Bemmelen PS, Beach K, Bedford G, Strandness Jr DE. The mechanism of venous valve closure: its relationship to the velocity of reverse flow. *Arch Surg* 1990;**125**:617—9.
22 Qui Y, Quijano RC, Wang SK, Hwang NH. Fluid dynamics of venous valve closure. *Ann Biomed Eng* 1995;**23**(6):750—9.
23 Kassab GS, Navia JA, Lu X. Proper orientation of the graft artery is important to ensure physiological flow direction. *Ann Biomed Eng* 2006;**34**(6):953—7.
24 Lu X, Kassab GS. Nitric oxide is significantly reduced in ex vivo porcine arteries during reverse flow because of increased superoxide production. *J Physiol* 2004;**561**(2):575—82.
25 Labropoulos N, Leon L, Kwon S, Tassiopoulos A, Gonzalez-Fajardo JA, Kang SS, et al. Study of the venous reflux progression. *J Vasc Surg* 2005;**41**(2):291—5.